Vision Research 149 (2018) 86–101

Contents lists available at ScienceDirect

Vision Research

journal homepage: www.elsevier.com/locate/visres

Dark scene elements strongly influence cuttlefish camouflage responses in visually cluttered environments

C. Chubb[a,c,*], C.-C. Chiao[b,c], K. Ulmer[c], K. Buresch[c], M.A. Birk[c], R.T. Hanlon[c]

[a] Department of Cognitive Sciences and Institute for Mathematical Behavioral Sciences, University of California at Irvine, Irvine, CA, USA
[b] Department of Life Science and Institute of Systems Neuroscience, National Tsing Hua University, 101, Sec 2, Kuang Fu Road, Hsinchu 30013, Taiwan
[c] Marine Biological Laboratory, Woods Hole, MA, USA

ARTICLE INFO

Number of reviewers = 2

Keywords:
Cephalopod
Sensorimotor system
Dynamic camouflage
Disruptive body pattern
Sepia officinalis
Gray-scale scrambles

ABSTRACT

This study investigated how cuttlefish (*Sepia officinalis*) camouflage patterns are influenced by the proportions of different gray-scales present in visually cluttered environments. All experimental substrates comprised spatially random arrays of texture elements (texels) of five gray-scales: *Black*, *Dark gray*, *Gray*, *Light gray*, and *White*. The substrates in Experiment 1 were densely packed arrays of square texels that varied over 4 sizes in different conditions. Experiment 2 used substrates in which texels were disks separated on a homogeneous background that was *Black*, *Gray* or *White* in different conditions. In a given condition, the histogram of texel gray-scales was varied across different substrates. For each of 16 cuttlefish pattern response statistics *c*, the resulting data were used to determine the strength with which variations in the proportions of different gray-scales influenced *c*. The main finding is that darker-than-average texels (i.e., texels of negative contrast polarity) predominate in controlling cuttlefish pattern responses in the context of cluttered substrates. In Experiment 1, for example, substrates of all four texel-sizes, activation of the cuttlefish "white square" and "white head bar" (two highly salient skin components) is strongly influenced by variations in the proportions of *Black* and *Dark gray* (but not *Gray*, *Light gray*, or *White*) texels. It is hypothesized that in the context of high-variance visual input characteristic of cluttered substrates in the cuttlefish natural habitat, elements of negative contrast polarity reliably signal the presence of edges produced by overlapping objects, in the presence of which disruptive pattern responses are likely to achieve effective camouflage.

1. Introduction

Cuttlefish are masters of rapid adaptive camouflage. In milliseconds, a cuttlefish can alter its body pattern to elude detection across a wide range of habitat variations (Hanlon & Messenger, 1988, 1996; Messenger, 2001). It is well documented that the pattern produced by a cuttlefish is controlled predominantly by the visual input it receives from its surroundings (Hanlon & Messenger, 1988; Holmes, 1940; Marshall & Messenger, 1996), and substantial research has sought to understand the algorithm that takes environmental image data as input and produces a camouflage skin pattern as output (Allen, Mäthger, Barbosa, & Hanlon, 2009; Allen et al., 2010, 2003; Barbosa, Litman, & Hanlon, 2008a, 2008b; Barbosa et al., 2007, Barbosa, Allen, Mäthger, & Hanlon, 2012; Barbosa et al., 2007; Buresch et al., 2011; Chiao, Chubb, Buresch, Siemann, & Hanlon, 2009; Chiao & Hanlon, 2001a, 2001b; Chiao, Chubb, & Hanlon, 2007; Chiao, Kelman, & Hanlon, 2005; Chiao et al., 2010, 2013; Hanlon, 2007; Hanlon, Chiao, Mathger, & Marshall, 2013; Hanlon et al., 2009, 2011; Kelman, Baddeley, Shohet, & Osorio, 2007; Kelman, Osorio, & Baddeley, 2008; Marshall & Messenger, 1996; Mäthger, Barbosa, Miner, & Hanlon, 2006; Mäthger et al., 2007; Shohet, Baddeley, Anderson, Kelman, & Osorio, 2006; Shohet, Baddeley, Anderson, & Osorio, 2007; Shohet et al., 2007; Tublitz, Gaston, & Loi, 2006; Zylinski & Osorio, 2011; Hanlon, 2007; Zylinski, Osorio, & Shohet, 2009a, 2009b; Zylinski, Darmaillacq, & Shashar, 2012).

1.1. The three main types of cuttlefish patterns

The patterns produced by cuttlefish fall into three main classes: uniform, mottle, and disruptive. Uniform (or uniformly stippled) body patterns show minimal variation in color and contrast; such patterns are typically deployed by cuttlefish to achieve general resemblance to homogeneous backgrounds such as sand. Mottle patterns consist of relatively fine-grained, medium-contrast texture that covers the cuttlefish dorsum more or less homogeneously; such patterns are typically deployed to achieve general resemblance to substrates with fine-

* Corresponding author at: Department of Cognitive Sciences and Institute for Mathematical Behavioral Sciences, University of California at Irvine, Irvine, CA, USA.
E-mail address: cfchubb@uci.edu (C. Chubb).

https://doi.org/10.1016/j.visres.2018.06.003
Received 10 November 2017; Received in revised form 3 June 2018; Accepted 4 June 2018

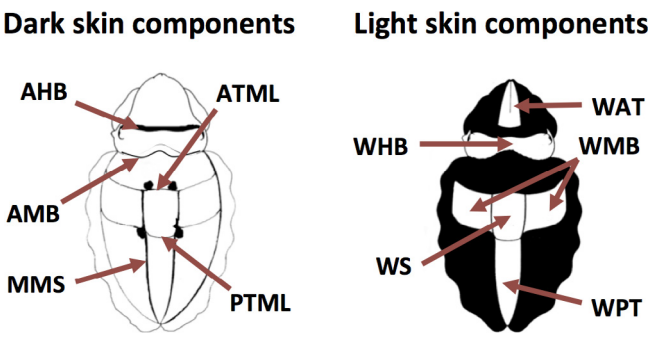

Fig. 1. Left: the five dark skin components that tend to be activated in disruptive coloration: AHB—anterior head bar, AMB—anterior mantle bar, ATML—anterior transverse mantle line, PTML—posterior transverse mantle line, and MMS—median mantle stripe. Right: the five light skin components that tend to be activated in disruptive coloration: WAT—white arm triangle, WHB—white head bar, WMB—white mantle bars, WS—white square, and WPT—white posterior triangle.

grained variations, e.g., regions composed of light and dark pebbles small in size relative to the cuttlefish (Chiao et al., 2010). Disruptive patterns are marked by highly salient, large, high-contrast skin components (as illustrated in Fig. 1) that are suppressed in uniform and mottle patterns. These elements tend to produce vivid edges, highly polarized in assigning one side to figure and the other to ground, that operate to fragment the cuttlefish into large chunks of visual "detritus"; such patterns are often deployed in visually cluttered environments comprising stones, shells, etc. whose sizes are comparable to the sizes of the large and differently oriented skin components that can be turned on and off selectively by the cuttlefish.

1.2. First-order image statistics and cuttlefish pattern responses

The current study aims to analyze how cuttlefish pattern responses are influenced by the first-order statistics (defined below) of the visual input in seven different cluttered contexts. All substrates used in this study are composed solely of different gray-scales. The current experiments ignore the possible influence of color because *Sepia officinalis* has only a single photopigment; thus, despite the surprisingly close color matches they sometimes achieve to substrates in their natural habitat, these animals seem to be colorblind (Marshall & Messenger, 1996; Mäthger et al., 2006; although see Stubbs A. L., 2015, for a theory of how they might sense color). In any case, even if *Sepia officinalis* is sensitive to color, substantial evidence suggests that variations in substrate intensity play a central role in controlling their pattern responses.

Experiment 1 analyzes four contexts composed of densely packed squares of different gray-scales; these contexts differ in spatial scale, i.e. in sizes of the square texture elements (texels) of which they are composed. Experiment 2 explores the influence of a basic aspect of context, the background gray-scale against which texels appear; in this experiment, circular texels are isolated against a background that is *Black*, *Gray*, or *White* in three different contexts.

A statistic extracted from an image is called a "first-order" statistic if its value is invariant with respect to spatial reordering of the elements composing the image. Thus, for example, (i) the mean gray-scale of an image is a first-order statistic because the value of the mean does not change no matter how one rearranges the pixels (or chunks) that make up an image. Other examples of first-order statistics are: (ii) the proportion of pixels in an image that have been assigned a given gray-scale, and (iii) the contrast of an image.

Because the statistical properties of cluttered scenes are largely invariant with respect to reordering of the homogenous chunks of which they are composed, one might expect first-order statistics to play an important role in controlling pattern responses in such contexts. To our knowledge, however, this issue has never before been investigated.

The specific purpose of the current experiments is to determine how each of 16 skin pattern statistics is influenced by different gray-scales in various cluttered contexts. Ten of these statistics are the activation levels of the 10 skin components illustrated in Fig. 1. We use statistics extracted automatically from the digitized image of the cuttlefish to estimate the activation of each of these 10 skin components in the pattern evoked by any given substrate. We also extract 6 additional image statistics; these "granularity spectrum coefficients" reflect the distribution of the image energy in the cuttlefish skin pattern across six different, isotropic spatial frequency bands.

1.3. The seven cluttered context substrates to be analyzed

The probability distribution that gives the proportions of the different gray-scales that make up a given, cluttered substrate S is called the histogram of S. We will write U for the uniform histogram that assigns equal probability to each of the five gray-scales g = *Black*, *Dark gray*, *Gray*, *Light gray*, *White*; that is, $U(g) = U(g) = \frac{1}{5}$.

The particular histogram U will play a central role in the experiments reported here. Specifically, each of the seven "context substrates" analyzed in this study comprises a spatially random array of texture elements (texels) with equal proportions of five gray-scales: *Black*, *Dark gray*, *Gray*, *Light gray*, and *White*. That is, the gray-scales of the texels in each of our 7 context substrates have histogram U. For example, one of the contexts that will be analyzed is the substrate $S_{1,\ 100\%}$ (Fig. 3) composed of a dense array of square texels equal in area to the WS of an average-sized cuttlefish subject; the gray-scales of the squares in $S_{1,100\%}$ have histogram U, and the spatial arrangement of gray-scales is random. In addition to $S_{1,100\%}$, we will analyze six other substrates. Like $S_{1,100\%}$, substrates $S_{1,50\%}$, $S_{1,30\%}$, and $S_{1,10\%}$ (Fig. 3), comprise densely packed, square texels; however, the texels in these substrates are smaller than the texels in $S_{1,100\%}$. Specifically, for K = 50, 30, 10, the area of a texel in $S_{1,K\%}$ is equal to $K\%$ of the area of the WS of a typical cuttlefish subject. The four context substrates $S_{1,100\%}$, $S_{1,50\%}$, $S_{1,30\%}$, and $S_{1,10\%}$ will be analyzed in Exp. 1. Three additional context substrates, $S_{1,Black}$, $S_{1,Gray}$ and $S_{1,White}$ will be analyzed in Exp. 2. In each of these substrates, texels are circular, equal in area to the WS of a typical cuttlefish subject, and separately individuated on a homogeneous background. In substrate $S_{1,Black}$ the gray-scale of this background will be *Black*; in substrate $S_{1,Gray}$ the gray-scale of this background will be *Gray*, and in substrate $S_{1,White}$ the gray-scale of this background will be *White*.

1.4. The strategy of the experiments

To analyze how pattern responses are influenced by different gray-scales in any given context $S_{1,X}$ for X = 100%, 50%, 30%, 10% (in Experiment 1) or *Black*, *Gray*, or *White* (in Experiment 2), we must test cuttlefish on substrates whose histograms deviate from U, the histogram of the context substrate $S_{1,X}$. Consider the context substrate, $S_{1,100\%}$, for example: testing cuttlefish on $S_{1,100\%}$ would enable us to measure the average pattern response evoked by $S_{1,100\%}$; however, this observation alone would not inform us of the relative influence of different gray-scales in evoking this response. To gain insight into this deeper issue, we must vary the proportions of different gray-scales in our test substrates and see how these variations affect the response pattern of the cuttlefish.

Examples of the different substrates used in both experiments are shown in Fig. 2. The bar graph associated with a row of substrates in Fig. 2 shows the texel gray-scale histogram of the substrates in that row. This set of histograms is sufficiently rich to enable us to fully characterize the differential effectiveness with which the different gray-scales *Black*, *Dark gray*, *Gray*, *Light gray*, and *White* influence any one of the 16 image statistics that we use to characterize the response pattern of a cuttlefish. The key property enabling full characterization is that the 9 histograms of these substrates span the space of all real-valued

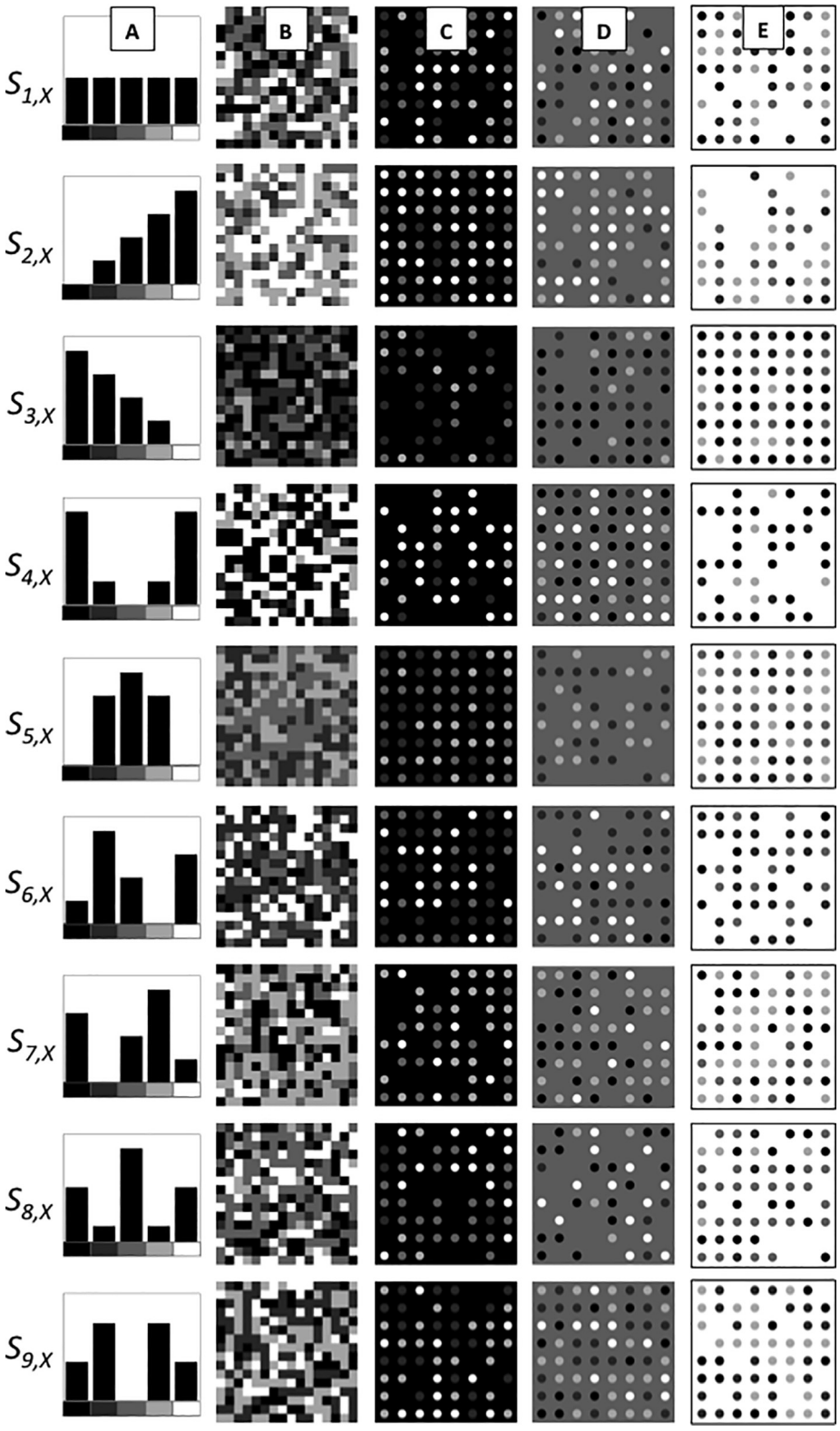

Fig. 2. *The gray-scale scrambles used in Exps. 1 and 2.* The bar graphs in Column A show the histograms of the substrates in the corresponding row. For $k = 1, 2,\ldots, 9$, column B shows dense scrambles $S_{k,X} = S_{k,100\%}$ (Experiment 1). Columns C, D and E show sparse scrambles $S_{k,X} = S_{k,Black}$, $S_{k,Gray}$, and $S_{k,White}$ (Experiment 2).

functions of the set {*Black*, *Dark gray*, *Gray*, *Light gray*, *White*}. In addition, however, for $X = 100\%, 50\%, 30\%, 10\%$, *Black*, *Gray*, or *White*, we force our conditions to be symmetric with respect to the context substrate, $S_{1,X}$. Note, for example, that the histograms of substrates $S_{2,X}$ and $S_{3,X}$ are complementary in the sense that their average is equal to U (the histogram of substrate $S_{1,X}$); the same is true of the histograms of substrates (a) $S_{4,X}$ and $S_{5,X}$, (b) $S_{6,X}$ and $S_{7,X}$, and also (c) $S_{8,X}$ and $S_{9,X}$. Thus, for $i = 2, 4, 6, 8$, substrates $S_{i,X}$ and $S_{i+1,X}$ result from symmetrically opposed perturbations of the substrate histogram away from U.[1]

[1] We note, however, that little is known about the low-level visual transformations

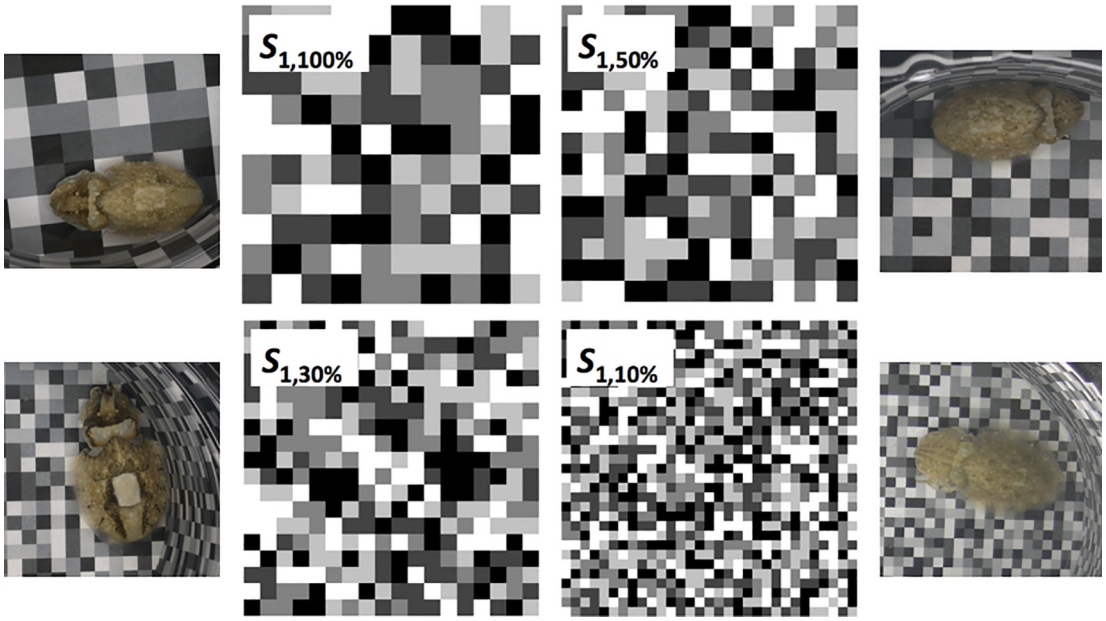

Fig. 3. The four different context substrates analyzed in Experiment 1. For X = 100%, 50%, 30%, 10%, texture elements (texels) in substrates $S_{1,X}$ have area equal to roughly X of the area of the white square of a typical cuttlefish subject. In each of these substrates, the proportions of gray-scales *Black*, *Dark gray*, *Gray*, *Light gray* and *White* are equal. Side panels show cuttlefish subjects being tested on corresponding substrates.

For a given cuttlefish skin pattern statistic c, in a given context X = 10%, 30%, 50%, 100%, *Black*, *Gray*, *White*, our goal is to estimate a function that reflects the strength with which different gray-scales influence the statistic c across the 9 perturbations of the context substrate $S_{1,X}$. The model we use for this purpose is described in Eq. (1) below.

2. General materials and methods

2.1. Animals and experimental setup

Twenty-eight cuttlefish (*Sepia officinalis*) were used in the study. Cephalopods are invertebrates and not subject to USA guidelines; however, in accordance with the principle articulated in the in the Declaration of Helsinki that the welfare of animals used for research must be respected, the MBL staff veterinarian oversaw our animal colony, and no cuttlefish were touched, stressed or injured.

All cuttlefish ranged in size between roughly 5.5 and 7.5 cm. (mantle length). All animals were hatched, reared, and maintained at the MBL Marine Resources Center (Woods Hole, MA) from eggs collected in the wild in southern England. The environment in which they were reared was visually enriched with stones, plastic greenery and plastic half-pipes that afforded concealment. To minimize stress to the animals, and to standardize the visual environment, experimental trials were conducted inside a tent of black plastic sheeting. Each animal was placed in a tank (55 cm × 40 cm × 15 cm) with flowing seawater and restricted to a cylindrical arena (25 cm diameter, 11 cm height) where various computer-generated texture substrates (laminated to be waterproof) were presented on both the floor and wall. On each experimental trial, a given animal was transferred from its home tank, tested on a single substrate and then returned to its home tank. To limit transfer stress, each animal experienced at most two such trials per day. A circular 40 W fluorescent light source (Phillips CoolWhite) was used to reduce the effect of shadow. A light meter (Extech EasyView EA30) was used to take readings around the perimeter and near the center of the arena (center 1.07 klux; perimeter 1.03 klux), showing that the arena was lit relatively evenly. Once the animal had acclimated (i.e., ceased swimming and hovering movements and expressed a stable body pattern), three still images were taken at roughly 4 min intervals using a digital video camera (Panasonic PVGS400) mounted 60 cm above the arena and connected to an external monitor so that the animal's movements could be followed from outside the chamber without disturbing it. The 3 images per animal per substrate in each trial were used to quantify the animal's response (the automated methods for quantifying body patterns are described below).

3. Experiment 1 methods

A "gray-scale scramble" is a spatially random mixture of different texels varying in gray-scale in proportions that conform as precisely as possible to a specified probability distribution. To create an N-texel patch of scramble with a given histogram h, one fills a virtual container with N copies of different gray-scales conforming as closely as possible to histogram h, and then one assigns the gray-scales in the container randomly, without replacement to the locations in the patch.

The substrates used in Exp. 1 were various sorts of gray-scale scrambles composed of *Black*, *Dark gray*, *Gray*, *Light gray* and *White*. These five gray-scales were linearly spaced in reflectance. *Black* had reflectance ≈ 8.2%, and *White* had reflectance ≈ 99%. However, the lamination process used to produce substrates made the substrate surface non-lambertian. Thus, the luminance projected into the eye of a cuttlefish from a given *Black* texel depended on the angle of incidence of the cuttlefish line of sight to the laminated sheet at the texel location, with increasingly acute angles yielding weaker blacks. Nonetheless, as reflected by the results reported below, it is clear that all five gray-scales were visibly distinct for our cuttlefish subjects and indeed that *Black* texels played the most important role in controlling pattern responses. Examples of scrambles are shown in Fig. 2.

Each of Experiments 1 and 2 used scrambles with 9 histograms. These histograms are shown in Col. A of Fig. 2. Column B of Fig. 2 shows the corresponding scrambles (for a single texel-size) used in Experiment 1. (Columns C, D and E show the corresponding substrates used in Experiment 2.) For X = 100%, 50%, 30%, 10% (Experiment 1)

(*footnote continued*)
applied by the visual system of the cuttlefish to the retinal input. Substrates $S_{4,X}$ and $S_{5,X}$ have equal mean reflectance; this should not be taken to imply, however, that these two substrates produce equal space-average activation in the cuttlefish visual system at any level of processing.

or *Black*, *Gray*, or *White* (Experiment 2), substrate $S_{1,X}$ has uniform histogram *U*. $S_{2,X}$ has a histogram that assigns linearly increasing probability to the five gray-scales ranging from *Black* to *White*, and $S_{3,X}$ has the complementary histogram that assigns linearly decreasing probability. Substrates $S_{4,X}$ and $S_{5,X}$ also have complementary histograms, as do substrates $S_{6,X}$ and $S_{7,X}$ and substrates $S_{8,X}$ and $S_{9,X}$.

Experiment 1 also varied the texel-area of the scrambles on which cuttlefish were tested. The coarsest scrambles had texels whose area was approximately 100% of the area of the white square of a cuttlefish subject (WS-area). Other conditions used scrambles whose texels had area equal to 50%, 30% and 10% WS-area. Examples of substrate $S_{1,X}$, for X = 50%, 30% and 10% are shown in Fig. 3. In addition, the side panels of Fig. 3 show cuttlefish subjects being tested on the corresponding substrates.

3.1. Animal subjects used in Experiment 1

10 cuttlefish were tested on all nine of the substrates with texel-area = 100% WS-area. Due to attrition, only nine of these cuttlefish were tested on the substrates with texel-area = 30% WS-area, and only eight were tested on the substrates with texel-area = 50% WS-area. Eight different cuttlefish were tested on the substrates with texel-area = 10% WS-area.

3.2. Quantification of the strength of skin component activation

The current study focuses primarily on the five light and five dark skin components that are responsible for disruptive coloration in *S. officinalis* (Hanlon & Messenger, 1988). These skin components are illustrated in Fig. 1. The five dark skin components are shown on the left. These are the anterior head bar (AHB), the anterior mantle bar (AMB), the anterior transverse mantle line (ATML), the posterior transverse mantle line (PTML), and the median mantle stripe (MMS). The five light skin components are shown on the right. These are the white arm triangle (WAT), the white head bar (WHB), the white mantle bars (WMB), the white square (WS), and the white posterior triangle (WPT).

We have described elsewhere (Chiao et al., 2009) the method we use to quantify the levels of activation evoked in the five light and five dark skin components illustrated in Fig. 1. This method requires that the experimenter interact with a Matlab program to (1) cut out the animal image to be analyzed from the background on which it appears and (2) indicate within the animal image several points that correspond to specific landmark points in a "standard" cuttlefish image. Following these image registration operations, the analysis proceeds automatically to extract all of the image statistics reflecting the activations of different skin components.

3.3. Quantification of additional body pattern summary statistics

Cuttlefish patterns typically vary in their overall granularity. Uniform/stipple patterns are largely homogeneous in coloration, sometimes with very fine-grained texturing; at the other extreme, disruptive patterns are marked by high activation of the coarse, light and dark skin components shown in Fig. 1; by contrast to both of these other pattern classes, mottle patterns show relatively fine- to medium-grained variation that fills the dorsum with texture that is largely homogeneous in quality (Hanlon et al., 2009).

To capture these overall patterning tendencies, in addition to gauging the activation of individual skin components in a cuttlefish camouflage pattern, our automated analysis also extracts summary measures that reflect the overall coarseness vs. fineness of the pattern (see Barbosa et al., 2008b for details). We gauge such differences in pattern granularity by analyzing the animal image into six, octave-wide, isotropic spatial frequency bands. Applying these six filters to the cuttlefish image yields six images that partition the information in the original image into different "granularity bands" (discarding a small amount of information in the highest and lowest frequencies).

From each of the six band-pass filtered images, we extract the sum of the squared pixel values in that image; this is the total contrast energy of the original, standardized image in the given spatial frequency band. These six contrast energies compose the "granularity spectrum" of the image, which is typically displayed as a curve. The scale of these numbers is arbitrary. We use a scheme in which contrast energy is expressed as a mean quantity per pixel and is normalized to reflect a proportion of the maximum possible contrast energy that could exist in any image. Based on the shape of this granularity spectrum, three major body patterns (uniform/stipple, mottle, and disruptive patterns) can be readily distinguished (Barbosa et al., 2008b). Typically, the spectrum of the uniform/stipple response has low contrast energy in all six granularity bands. The mottle pattern yields a spectrum with more contrast energy at all bands than the uniform/stipple pattern, and this spectrum has highest contrast energy in granularity bands 3 and 4. Finally, the disruptive pattern evokes a spectrum with more total contrast energy than either the uniform/stipple or mottle patterns, and most of this contrast energy is in the two coarsest granularity bands 1 and 2.

3.4. Modeling

The aim of the current experiments is to determine how different gray-scales operate to influence cuttlefish pattern responses in each of our seven cluttered context substrates. The response production process begins when the cuttlefish receives in its field of view a sample of texels of different gray-scales from the substrate. The neural circuitry that connects the retina of the cuttlefish to the skin component *c* (Fig. 1) performs a host of complicated computations that have been designed by evolution to achieve effective camouflage. Indeed, the various patterns of texels that might stimulate the retina of a cuttlefish from a particular substrate $S_{k,X}$ may produce variable levels of activation in *c*. However, the spatial randomness of our stimuli insures that, on average, across different test trials, the relative numbers of different gray-scales in the stimulus are likely to predominate in controlling *c*-activation. It is this dependency between gray-scales and *c*-activation that we seek to discover.

For the moment, let us consider a particular skin pattern statistic *c* of a particular cuttlefish *j* in a particular context *X*. For example, *c* might be the white square, *j* might be cuttlefish #3, and *X* might be the 30% context.) As illustrated in Fig. 4, the basic model we use here is very simple: it assumes that texels of different gray-scales in context *X*

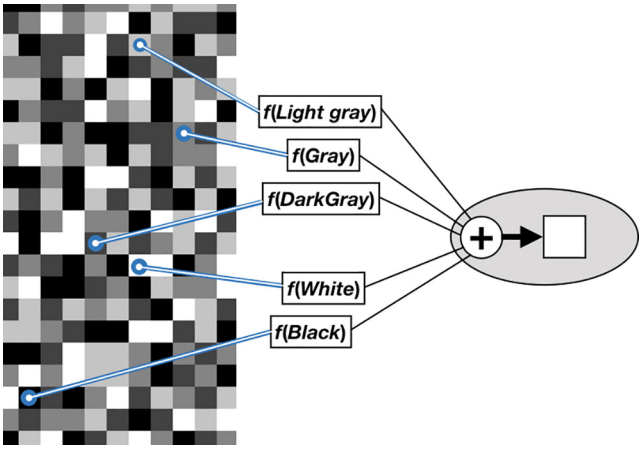

Fig. 4. The basic model. The ellipse represents a cuttlefish. The white square represents a skin component *c* (e.g., the WS of the cuttlefish). The model assumes that the activation of skin component *c* is determined by summing the influences of all the texels that the cuttlefish sees. For any gray-scale *g* = *Black*, *Dark gray*, *Gray*, *Light gray*, *White*, the *c*-influence function *f*(*g*) gives the influence exerted on *c*-activation in the cuttlefish by a texel of gray-scale *g*.

influence *c*-activation additively: Each texel that projects to the retina of the cuttlefish is assumed to nudge *c*-activation by an amount $f(g)$ (which may be either positive or negative) that depends on the gray-scale g of the texel.

Our first step is to use the data from cuttlefish j in context X to estimate $f(g)$ for g = *Black*, *Dark gray*, *Gray*, *Light gray*, *White*. In context X, the cuttlefish is tested on the 9 substrates $S_{k,X}$, $k = 1,2,\ldots,9$. Suppose that the *c*-activation evoked in cuttlefish j by substrate $S_{k,X}$ is A_k.[2] We seek the function $f(g)$ that best predicts all 9 *c*-activations A_k in the nine equations,

$$A_k = \sum_g f(g)h_k(g) + error_k. \quad k = 1, 2, \ldots, 9 \tag{1}$$

Specifically, we use linear regression to find $f(g)$ minimizing

$$\sum_{k=1}^{9} error_k^2. \tag{2}$$

This function $f(g)$ is called the *c*-influence function for cuttlefish j in context X. Thus, $f(g)$ is optimal (in a least-squares sense) for predicting the different levels of *c*-activation evoked in j by the substrates $S_{k,X}$, $k = 1,2,\ldots,9$ from their gray-scale histograms, $h_k(g)$, $k = 1, 2,\ldots, 9$.

The 9 histograms $h_k(g)$ include approximately equal total variation in the proportion of texels with any given gray-scale g; this constrains our estimate of the function $f(g)$ with roughly equal statistical power for all five gray-scales g. Our design thus allows us to treat the values $f(g)$, g = *Black*, *Dark gray*, *Gray*, *Light gray*, *White* as repeated measures in a standard, within-subjects analysis of variance for the particular set of cuttlefish j tested on the substrates $S_{k,X}$, $k = 1,2,\ldots,9$.

We would also like to test the null hypothesis that the responses of our cuttlefish subjects in a given context are controlled exclusively by the first-order statistics of the scrambles in that context. For this purpose, we use the four statistics Qk given in Eq. (3). Note that for $k = 1,2,3,4$, the complementarity of the histograms h_{2k} and h_{2k+1} implies that the four variables

$$Q_k = A_{2k} + A_{2k+1} \quad k = 1, 2, 3, 4, \tag{3}$$

should all have mean equal to two times the average value of the function f . Thus, if the four statistics Q_k show a significant degree of shared variation across the cuttlefish tested in a given context, then we must conclude that their responses in that context are influenced by factors other than variations in the proportions of different gray-scales.

4. Experiment 1 results

The fact that different cuttlefish were tested in different conditions limits the inferences that the results will support. In particular, for any given context X, and any given skin component (or granularity coefficient) c, we will restrict our computational analysis to the data from only those cuttlefish tested on the substrates of context X.

It should also be noted that the results for different skin pattern statistics c are likely to be highly correlated. For example, strong activation of the white square is frequently accompanied by strong activation of the white head bar. Thus, it is to be expected that the results shown in the panels in Fig. 5 for the white square and the white head bar will show similar patterns.

Images showing a single response pattern produced by each cuttlefish subject to each of substrates $S_{k,X}$, $k = 1, 2,\ldots, 9$, X = 100%, 50%, 30%, 10% are included in the supplementary materials.

Figs. 5 and 6 show the results for the dark and light skin components (Fig. 1). Each row of panels gives the results for one skin component in the X = 10%, 30%, 50% and 100% contexts. The curve plotted in the panel for skin component c and context X shows the average *c*-influence function (across all cuttlefish j tested in context X). The error bars, however, exclude variation due to differences in the average *c*-activation evoked in different cuttlefish j in context X; instead, the error bars reflect variations in the patterns of deviation of the individual *c*-influence functions from their means.

The units of the ordinate values for different rows of panels in Figs. 5, 6, 10 and 11 are arbitrary and not comparable across rows; only the relative values within a given row of panels should be considered.

4.1. The summary statistics "% variance" and "p."

Each panel in Figs. 5 and 6 is marked with two numbers, "*% variance*" and "*p*." These two numbers both reflect the strength with which the data for the given panel support the conclusion that the skin component c is activated more strongly by some gray-scales than by others in response to scrambles in context X.

The first number, "*% variance*," gives the percent of the total variance in *c*-activation across all animals that is due to a shared pattern of gray-scale influence. More specifically, for any cuttlefish j, let μ_j be the mean (across all five gray-scales g) of j's *c*-influence function $f_j(g)$ in context X, and let

$$\delta_j(g) = f_j(g) - \mu_j. \tag{4}$$

In addition, let $\bar{\delta}(g)$ be the average of the functions $\delta_j(g)$ across all cuttlefish j tested in context X. Thus, $\bar{\delta}(g)$ reflects the shared component of the individual cuttlefish fluctuation patterns. Then

$$\%variance = 100 \times \frac{V_{shared}}{V_{total}} \tag{5}$$

where

$$V_{Total} = \sum_{\substack{cuttlefish \\ j}} \sum_{\substack{grayscales \\ g}} \delta_j(g)^2 \tag{6}$$

and V_{shared} is the total variance accounted for by the shared fluctuation pattern, $\bar{\delta}(g)$: i.e.,

$$V_{shared} = V_{total} - \sum_{\substack{cuttlefish \\ j}} \sum_{\substack{grayscales \\ g}} (\delta_j(g) - \bar{\delta}(g))^2. \tag{7}$$

Note that if the functions $\delta_j(g)$ are identical for all cuttlefish j, then $V_{shared} = V_{total}$, and *% variance* = 100. More generally, *% variance* will rise significantly above 0 only if the *c*-activation is controlled similarly in different cuttlefish by variations in the proportions of different gray-scales in context X.

The second number "*p*" in each panel gives the *p*-value from a within-subjects analysis of variance in which: the subjects are all of the cuttlefish j tested in context X; the repeated measures are the values assigned to the five gray-scales g by cuttlefish j's *c*-influence function in context X; and the null hypothesis asserts that $\bar{\delta}(g) = 0$ for all gray-scales g. In each case, the degrees of freedom are corrected (to compensate for deviations from sphericity) using Box's $\hat{\varepsilon}$ adjustment (as recommended by Maxwell & Delaney, 2000).

4.2. Comparing the relative influence of Black vs. White texels

To investigate the relative strength with which *Black* vs. *White* texels influence cuttlefish pattern responses in all seven contexts tested in Exps. 1 and 2, we performed two paired-samples *t*-tests for each pattern response statistic c in each context. One test asked whether *Black* texels exerted significantly stronger influence on c activation than *White* texels; the other test asked whether *White* texels exerted significantly stronger influence than *Black* texels. (Thus, at most one of these two tests could be significant for a given statistic c in a given context.)

[2] It should be noted that for any given skin component, the units in which the activations A_k, $k = 1,2,\ldots,9$ are recorded are arbitrary. As this implies, it is meaningless to compare activations across different skin components. However, activations can be meaningfully compared between animals and across different contexts for a given skin component.

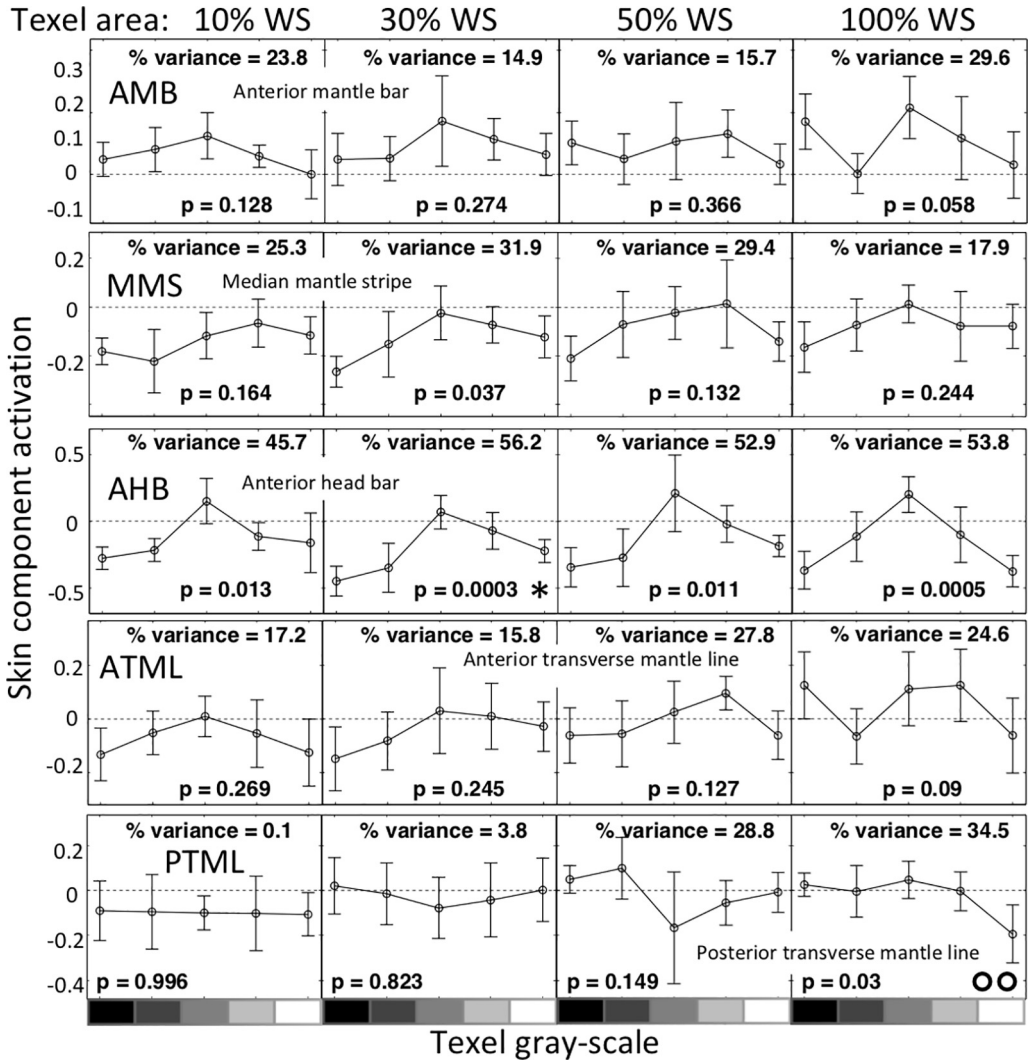

Fig. 5. Results from Experiment 1 for dark skin components. For a given skin component c and texel-area X, the curve plotted in the panel in row c and column X gives the average [across all cuttlefish tested on the 9 substrates with texel-area X] c-influence function $\overline{f}(g)$ for g = *Black*, *Dark gray*, *Gray*, *Light gray*, and *White*. Within each panel, more negative values indicate increased activation. Asterisks (circles) indicate that *Black* (*White*) texels influence c-activation significantly more strongly (* 0.01, oo 0.0031) than *White* (*Black*) texels. Error bars are 95% confidence intervals. The units on the y-axis are arbitrary and not comparable across different skin components. See text for description of "*% variance*" and "*p*."

Specifically, for each cuttlefish j tested in context X = 10%, 30%, 50% and 100%, let $D_j = f(Black) – f(White)$ where f is the c-influence function for cuttlefish j in context X. For the light skin components c (and also the granularity coefficients c), to test whether *Black* (*White*) texels exert stronger influence than *White* (*Black*) texels, we test the null hypothesis that the mean of the D_j's is significantly greater (less) than 0. Similarly, for the dark skin components c, to test whether *Black* (*White*) texels exert stronger influence than *White* (*Black*) texels, we test the null hypothesis that the mean of the D_j's is significantly less (greater) than 0. If a panel in any of Figs. 5–7, 9, 10 or 11 is marked with asterisks, this means that *Black* texels exert significantly stronger influence than *White* texels on c-activation at the 0.01 (∗) or 0.0031 (∗∗) level. (The Bonferroni correction for the 16 tests in a given context yields a critical value of 0.05/16 = 0.0031.) If a panel in any of Figs. 5–7, 9, 10 or 11 is marked with circles, this means that *White* texels exert significantly stronger influence than *Black* texels on c-activation at the 0.01 (o) or Bonferroni corrected 0.0031 (oo) level.

In considering Fig. 5, it is important to recognize that increased activation of a dark skin component c by texels of gray-scale g is signaled by a downward deflection of the c-influence function at g. Thus, for example, the relatively large negative values of the AHB-influence function at g = *White* and g = *Black* in the 100% context, indicate that increasing proportions of *Black* and *White* texels tend to activate the AHB.

The reverse is true in Fig. 6, which plots the results for the five light skin components. Heightened activation of a light skin component c by increasing proportions of a given gray-scale g is signaled by an upward deflection of the average c-influence function at g. For example, in the 100% context, the average WS-influence function assigns a large positive value to *Black*; this shows that the WS is strongly activated by *Black* texels in this context.

In Fig. 5 the skin component that is influenced most sensitively by different gray-scales is the anterior head bar (AHB), and in Fig. 6, two skin components stand out: the white head bar (WHB) and the white square (WS). The AHB seems to be activated with roughly equal strength by *Black* and *White* texels (at least in the 100% context). By contrast, *Black* texels are more effective than *White* texels in activating the WHB and the WS; this is true for all of the 10%, 30%, 50% and 100% contexts.

The results for the granularity spectrum coefficients c are shown in Fig. 7. Each row of panels in this figure gives the results for a single granularity spectrum band. The spatial frequencies collected in a given

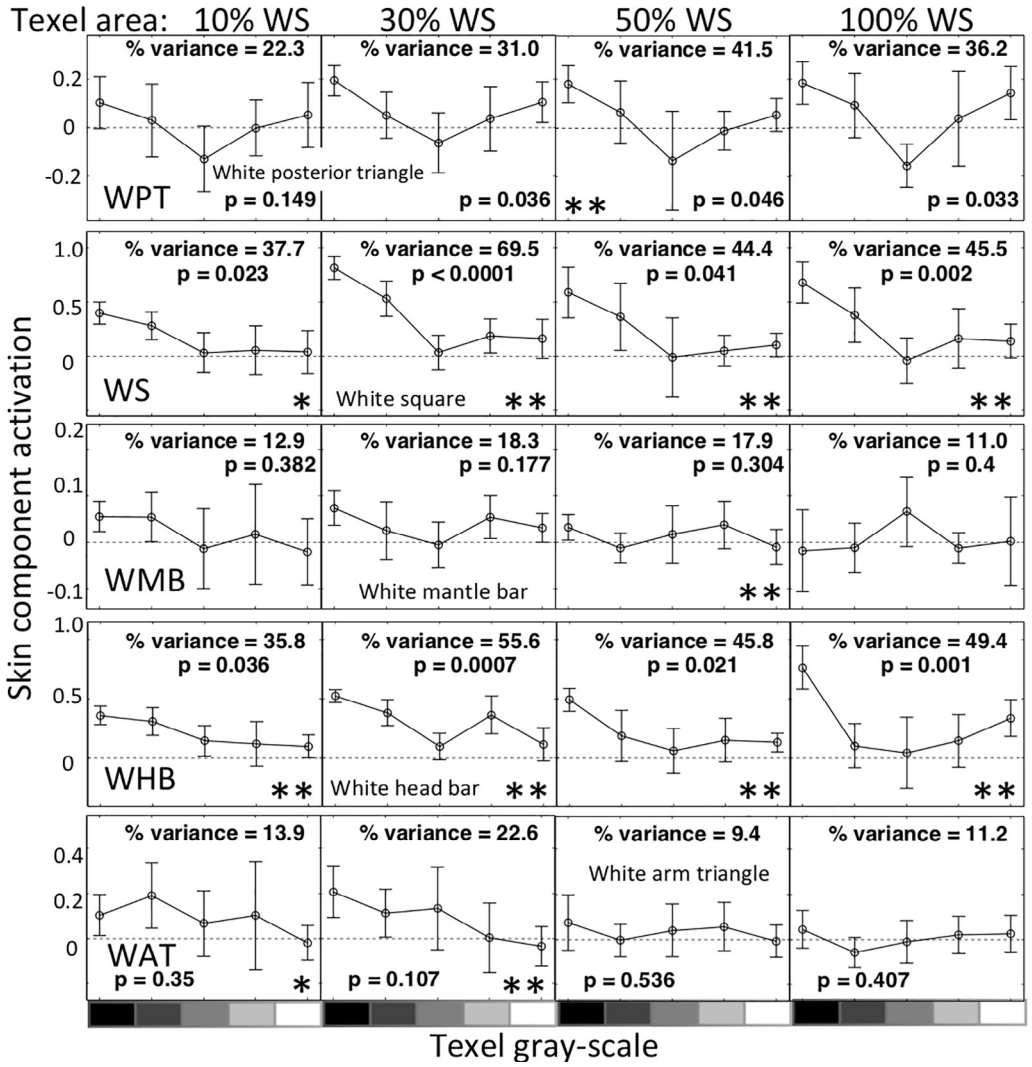

Fig. 6. *Results from Experiment 1 for light skin components*. For a given skin component *c* and texel-area *X*, the curve plotted in the panel in row *c* and column *X* gives the average [across all cuttlefish tested on the 9 substrates with texel-area *X*] *c*-influence function $\overline{f}(g)$ for g = *Black*, *Dark gray*, *Gray*, *Light gray*, and *White*. Within each panel, more positive values indicate increased activation. Error bars are 95% confidence intervals. Asterisks indicate that *Black* texels influence *c*-activation significantly more strongly (* 0.01, ** 0.0031) than *White* texels. The units on the *y*-axis are arbitrary and not comparable across different skin components. See text for description of "*% variance*" and "*p*."

band are suggested by the image of the filtered cuttlefish pattern at the right of the row. Successive columns of panels give results for the 10%, 30%, 50% and 100% contexts. A striking feature of this figure is that within a given column of panels, although they differ in amplitude, the *c*-influence functions for different granularity band coefficients *c* all take roughly the same form. For example, in the rightmost column of panels (for context $X = 100\%$), the *c*-influence functions for spatial frequency bands 1 through 6 all form symmetric "V's," showing equal sensitivity to gray-scales *White* and *Black* and also equal (but lower) sensitivity to gray-scales *Dark gray* and *Light gray* and minimal sensitivity to *Gray*. However, the amplitudes of the V-shaped *c*-influence functions for the 100% context are roughly equal in amplitude for granularity bands 1 and 2 (the two lowest frequency bands) and then decrease with increasing granularity band spatial frequency.

This same general pattern is evident for the granularity-band coefficients *c* in the 10%, 30% and 50% contexts as well; however, in each of these cases, the form of the *c*-influence function deviates from the clean symmetry observed in the 100% context. In particular, in the 30% context, the *c*-influence function shows higher sensitivity to *Black* than to *White* texels.

4.3. Testing for higher-order effects

To test the null hypothesis that the responses of our cuttlefish subjects are determined exclusively by variations in the gray-scale histograms of the scrambles in a given context, we perform a within-subjects analysis of variance in which: the subjects are all of the cuttlefish *j* tested in context *X*; the repeated measures are the four values Q_k given in Eq. (3) for the different cuttlefish *j*; and the null hypothesis asserts that the Q_k's for any cuttlefish deviate randomly from a flat line. In each case, the degrees of freedom are corrected (to compensate for deviations from sphericity) using Box's $\hat{\varepsilon}$ adjustment.

There was very little evidence of higher-order effects in any of the 10%-, 30%-, 50%- and 100%-contexts. For each of the 10%- and 30%-contexts, the test for higher-order effects yielded a *p*-value > 0.08 for all granularity coefficients and for all skin components. For the 50%-context, the test for higher-order effects yielded $p = 0.050$, 0.030 for granularity coefficients 1 and 2 and a $p = 0.045$ for the White Posterior Triangle; otherwise all *p*-values were > 0.06. Finally, in the 100%-context, the test for higher-order effects yielded $p = 0.038$ for granularity coefficient 3; otherwise, all *p*-values were > 0.05. A Bonferroni correction for the number of tests in a given context yields a critical

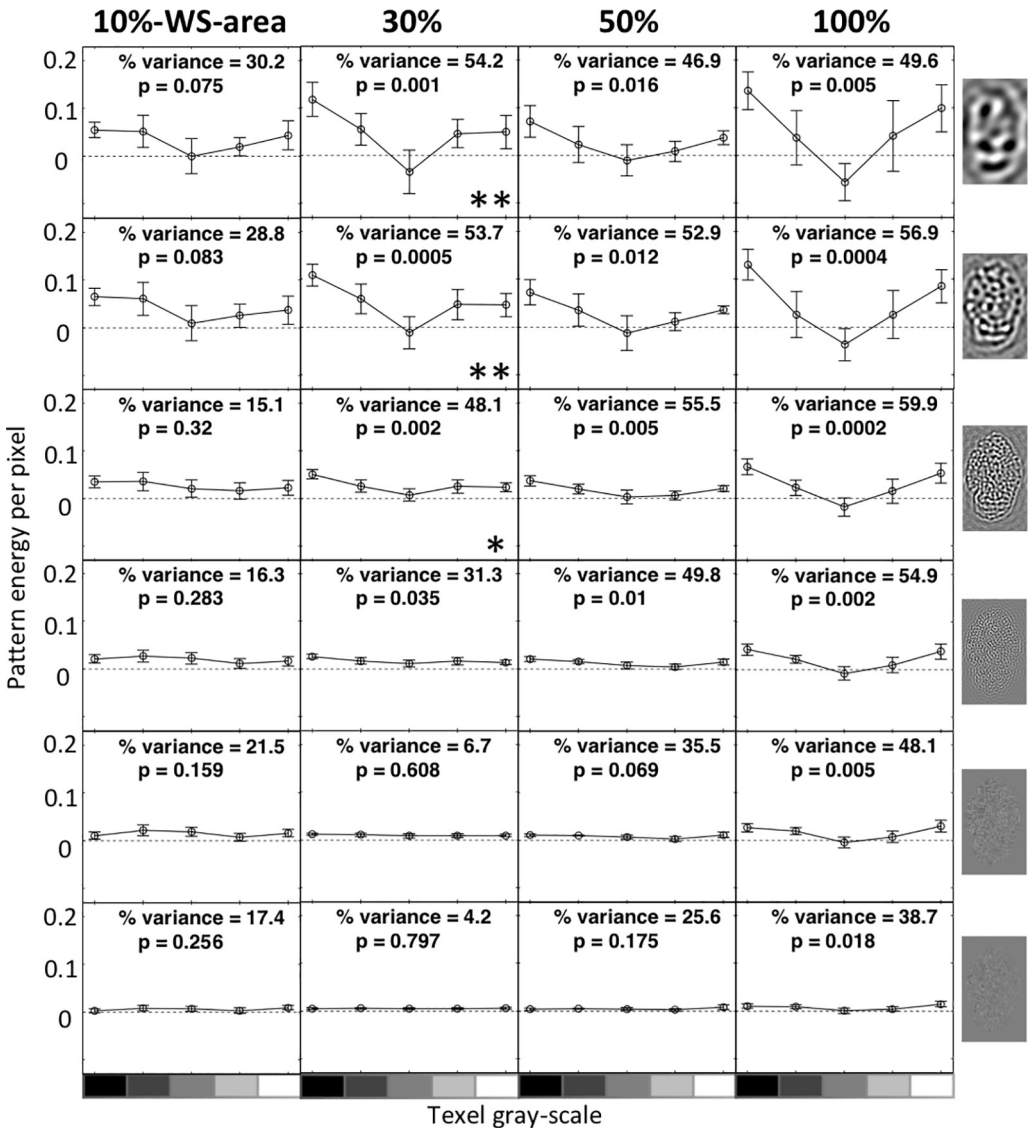

Fig. 7. *Results from Experiment 1 for the granularity spectrum coefficients.* For a given granularity band coefficient *c* and texel-area *X*, the curve plotted in the panel in row *c* and column *X* gives the average (across all cuttlefish tested on the 9 substrates with texel-area *X*) *c*-influence function $\overline{f}(g)$ for g = *Black*, *Dark gray*, *Gray*, *Light gray*, and *White*. Within each panel, more positive values indicate increased activation. Error bars give 95% confidence intervals. Asterisks indicate that *Black* texels influence *c*-activation significantly more strongly (* 0.01, ** 0.0031) than *White* texels. The spatial frequencies in a band are reflected by the image of the filtered cuttlefish pattern to the right of the row. See text for description of "*% variance*" and "*p*."

value of 0.05/16 = 0.0031 (where 16 is the number of pattern response statistics). None of the *p*-values observed in any of these tests was significant at this level. The current results are thus consistent with the model illustrated in Fig. 4.

5. Experiment 1 discussion

Perhaps the most striking feature of the results is the dominance of *Black* vs. *White* texels in controlling the activation of the five light skin components. This is shown by the asterisks that mark 12 of the 20 panels in Fig. 6 (and by the absence of circles in the figure).

By contrast, no such dramatic difference is evident either for the dark skin components (Fig. 5) or for the granularity coefficients (Fig. 7). Although Fig. 7 shows that *Black* texels are more effective than *White* texels in controlling the granularity spectrum coefficients 30% context, this is not true for any of the 10%, 50% or 100% contexts. In particular, it should be noted that the granularity spectrum coefficients in the 100% context are highly sensitive to variations in gray-scale histogram (as shown by the high values of "% variance" and the low values of "p" in this context); however, *White* and *Black* texels influence activation with equal effectiveness in this context.

As reflected by the "% variance" and "p" values in Figs. 5 and 6, three skin components are especially sensitive to variations in the gray-scales present in our scramble substrates. These are the anterior head bar (AHB) (a dark skin component), the white head bar (WHB) and the white square (WS) (light skin components). Other skin components (e.g., the white posterior triangle (WPT)) seem to show mild differential sensitivity to gray-scale for one or more of the 10%, 30%, 50% or 100% scrambles; however, in all of these other cases, the strength with which activation is controlled by variations in gray-scale composition is substantially lower than it is for the AHB, the WHB and the WS.

One might anticipate that the activation of the AHB would be likely to mimic the activation of the WHB; these two skin components abut each other and are often activated together. However, the *c*-influence function of the WHB differs from that of the AHB. This is especially clear for the 100% context. In this context, gray-scales *Black* and *White* influence AHB activation with equal effectiveness; however, *Black* exerts much more powerful influence than does *White* on WHB activation.

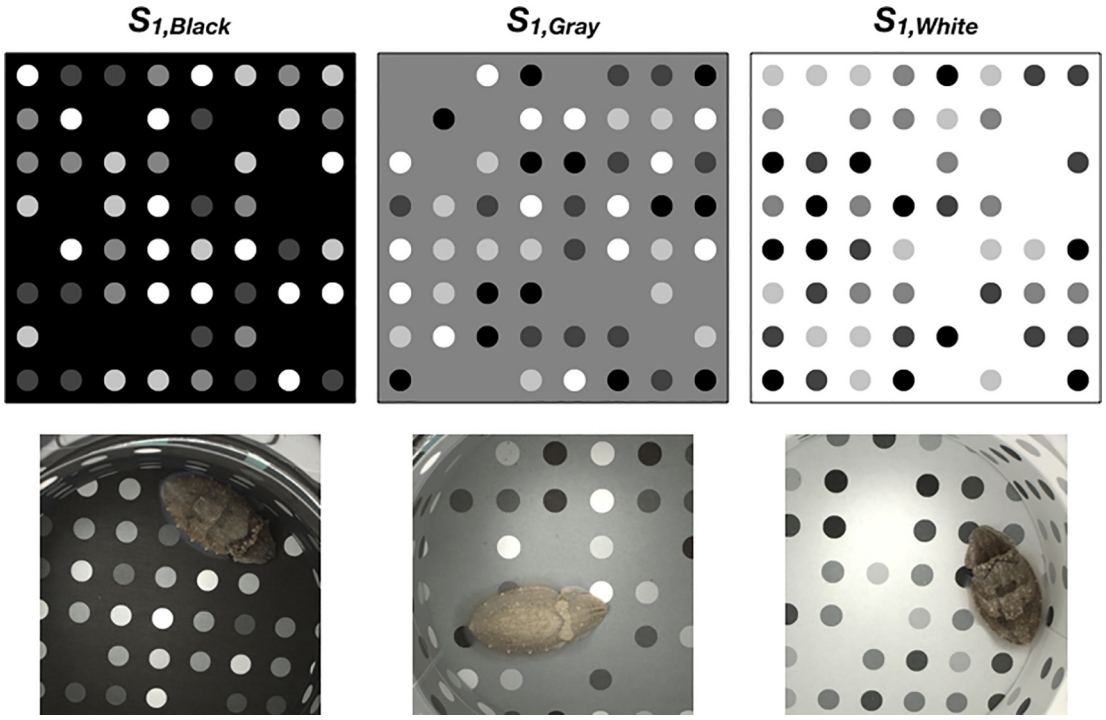

Fig. 8. The three different context substrates analyzed in Experiment 2. For X = *Black*, *Gray*, and *White*, texels are disks individually isolated against the background of gray-scale X. In each of these substrates, the proportions of gray-scales *Black*, *Dark gray*, *Gray*, *Light gray* and *White* are equal; however, in the substrate $S_{1,X}$, texels of gray-scale X are invisible, producing regions where texels appear to be missing. Associated panels show cuttlefish subjects being tested on corresponding substrates.

Strikingly, like the WHB, the WS is much more strongly influenced by *Black* than by *White* texels. This is true not only in the 100% context, but also in the 10%, 30% and 50% contexts as well.

There are, however, several notable deviations from this pattern, all of which occur in the 100% context. First (as noted above), the AHB-influence function in the 100% context is symmetric in its sensitivity to dark vs light texels. The same is true of the *c*-influence functions for the granularity spectrum coefficients c in the 100% context. (All of these functions are very similar in form.) These results might be taken to reflect a systematic difference in patterning strategy in the 100% context vs. the finer-grained contexts. However, we should not forget that even in the 100% context, the WS and WHB are much more strongly influenced by *Black* vs. other gray-scales.

In conjunction with previous findings, the current results dramatize the *context-dependent* nature of cuttlefish pattern responses. It has long been known that in the context of a mostly homogeneous black or gray background, white elements predominate in activating the skin components deployed in disruptive pattern responses (Chiao, Chubb, & Hanlon, 2015; Chiao & Hanlon, 2001a, 2001b). By contrast, the current results show that in densely cluttered backgrounds of variable gray-scale, black elements predominate in controlling the activation of these same skin components. In the context of a mostly homogeneous background comprising a few white items, a highly activated WS may masquerade as yet another of these white items, enabling the cuttlefish to escape detection. A highly cluttered substrate, however, may well afford other, potentially more effective, concealment strategies (some of which will be described in the general discussion). There is thus no reason to suppose that response patterns are controlled by the same image statistics in these two different contexts.

6. Experiment 2 methods

All of the scrambles studied in Experiment 1 were densely packed; one feature of such textures is that any individual texel t occurs in a complicated, random context that may well influence the impact t exerts on the cuttlefish pattern response. The four texels that share a side with a given texel t may take any combination of our five gray-scales. For a given skin component c, it is likely that the influence exerted on c-activation by t depends not only on the gray-scale of t, but also on the configuration of texels that form t's context. If t is *Black*, for example, then it seems plausible to expect that t will exert a stronger influence on c-activation if it is surrounded exclusively by *White* texels (rendering t highly salient) than if t is surrounded by a mixture of *Dark gray* and *Black* texels.

The purpose of Experiment 2 is to determine how the impact exerted on pattern responses by different gray-scales is affected by a basic aspect of context: the background gray-scale against which texels appear. In this experiment, every texel occurs in isolation against a homogeneous background. In three different conditions, the background is *White*, *Gray*, or *Black*. In all cases, texels are disks arranged in a square array.

The basic contexts $S_{1,Black}$, $S_{1,Gray}$, and $S_{1,White}$ (i.e., the substrates in which texels of all 5 gray-scales occur with equal probability) are shown in Fig. 8. Associated with each context substrate is an image of a cuttlefish being tested on that substrate.

The substrates used in Experiment 2 are shown in Columns C, D and E of Fig. 1. Scramble histograms are shown in Column A of Fig. 1. Corresponding *White*-background, *Gray*-background and *Black*-background scrambles are shown in Columns C, D and E. In all of the substrates used in Experiment 2, the area of each circular texel was approximately equal to the average area of the WS of our cuttlefish subjects. In some substrates there appear to be gaps where texels are missing. This effect is due to the fact that the disks occupying those locations have the same gray-scale as the background.

7. Experiment 2 results

Images showing a single response pattern produced by each cuttlefish subject to each of substrates $S_{k,X}$, k = 1, 2,…, 9, X = *Black*, *Gray*, *White* are included in the supplementary materials.

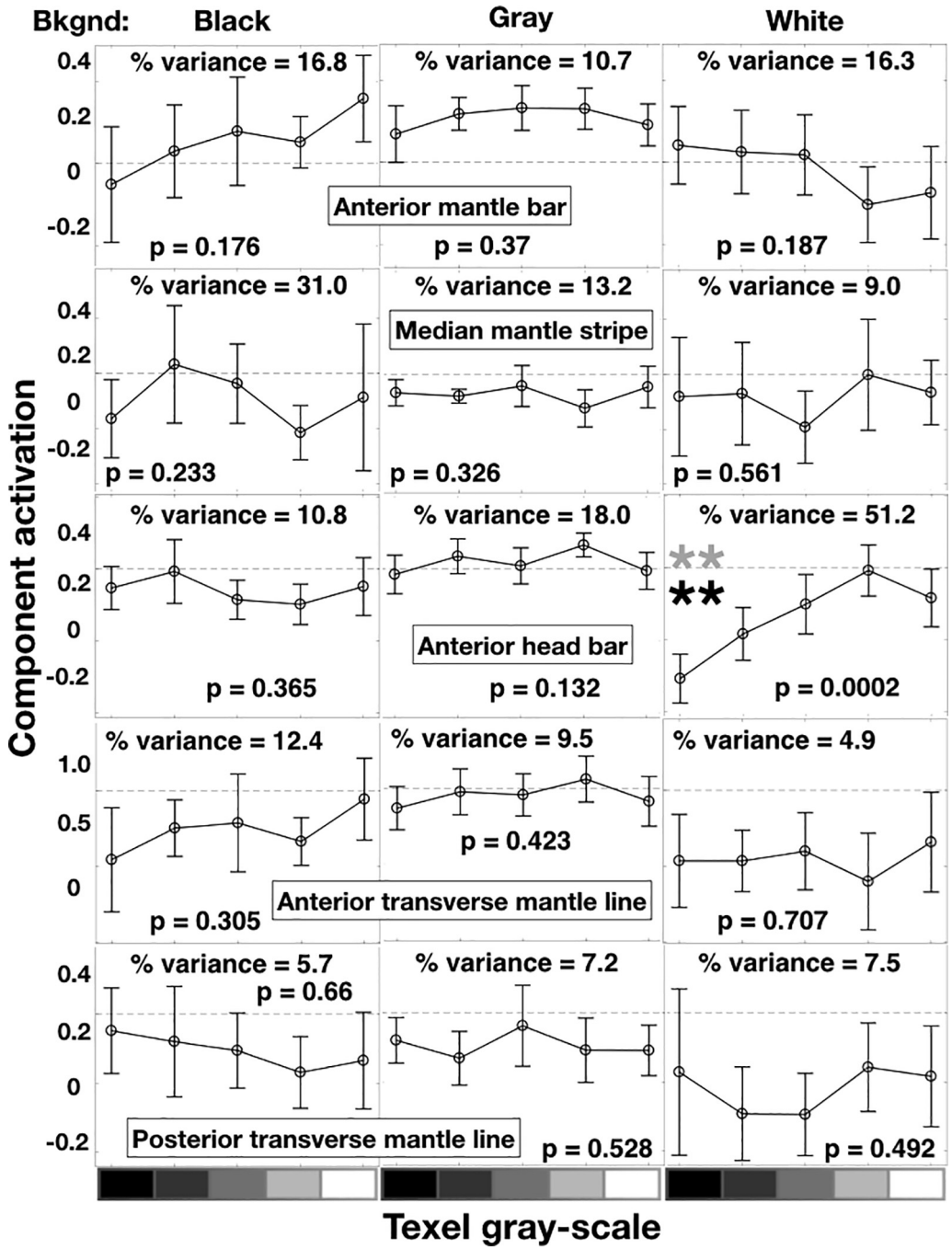

Fig. 9. Results from Experiment 2 for dark skin components. For a given skin component *c* and background gray-scale *X*, the curve plotted in the panel in row *c* and column *X* gives the average *c*-influence function $\overline{f}(g)$ for g = *Black*, *Dark gray*, *Gray*, *Light gray*, and *White*. Within each panel, more negative values indicate increased sensitivity. Error bars are 95% confidence intervals. Black (gray) "**" indicates that *Black* texels influence *c*-activation more strongly than *White* (*Light gray*) texels at the 0.0031 significance level. See "*Experiment 1 results*" for description of "*% variance*" and "*p*."

Figs. 9–11 show the results for dark skin components, the light skin components, and the granularity spectrum coefficients respectively. Each row of panels gives the results for one pattern-response statistic *c* across the substrates with *X* = *Black*, *Gray* and *White* backgrounds from left to right. Included in the panel for pattern-response statistic *c* in context *X* is the average *c*-influence function (for all cuttlefish tested in context *X*) as well as the two statistics, %-variance and *p*, described in *Experiment 1 results*. In addition, if a panel contains a single black "∗" ("o"), this indicates that *Black* (*White*) texels influence *c*-activation more strongly than *White* (*Black*) texels at the 0.01 significance level (as reflected by a paired-samples *t*-test); "∗∗" or "oo" indicates that the result is significant at the (Bonferroni-corrected) level of 0.0031.

In addition, panels in the third column of each of Figs. 9–11 may be marked with either one or two gray asterisks or circles. The results plotted in column 3 are for the *White*-background context. In this context, *White* texels disappear into the background; thus, the lightest texels that appear as disks are the *Light gray* ones. The gray asterisks and circles reflect the results of paired-samples *t*-tests comparing the influence exerted by *Black* vs. *Light gray* texels in this context.

7.1. Dark skin components

There is little evidence that gray-scales differentially influence the activation of any dark skin components on backgrounds *X* = *Black* or

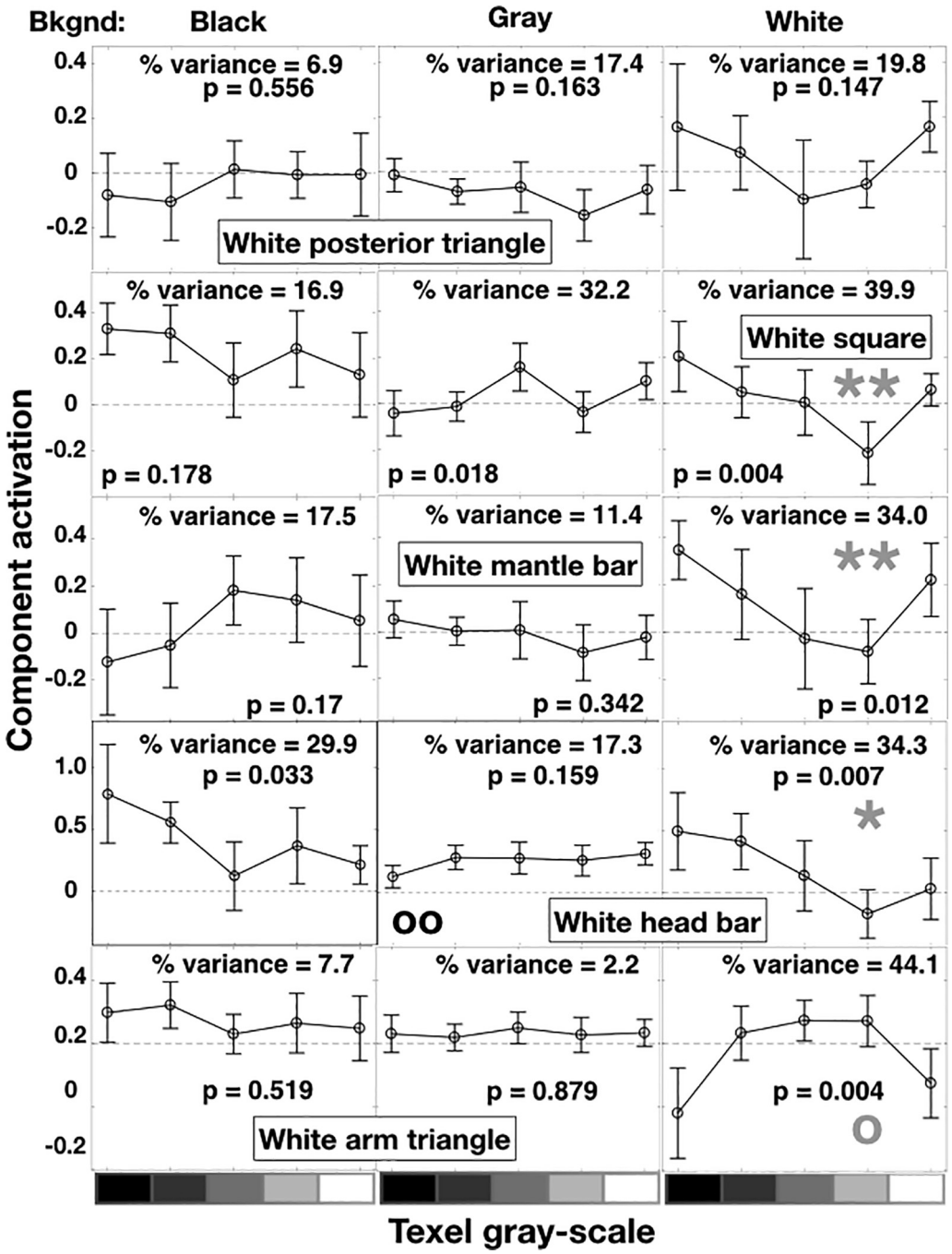

Fig. 10. *Results from Experiment 2 for light skin components*. For a given skin component *c* and background gray-scale *b*, the curve plotted in the panel in row *c* and column *b* gives the average *c*-influence function $\overline{f}(g)$ for *g* = *Black*, *Dark gray*, *Gray*, *Light gray*, and *White*. Within each panel, more positive values indicate increased sensitivity. Error bars are 95% confidence intervals. Black "oo" (Gray "o") indicates that *White* (*Light gray*) texels influence *c*-activation more strongly than *Black* texels at the 0.0031 (0.01) significance level. Gray "**" ("*") indicates that *Black* texels influence *c*-activation more strongly than *Light gray* texels at the 0.0031 (0.01) significance level. See "*Experiment 1 results*" for description of "*% variance*" and "*p*."

X = *Gray*. On background *X* = *White*, however, AHB-activation is influenced significantly by variations in gray-scale histogram ($p = 0.0002$); in particular, AHB-activation is influenced significantly more strongly by *black* texels than by either *Light gray* or *White* texels.

7.2. Light skin components

Aside from the fact that *White* texels exert significantly stronger influence on WHB activation than do *Black* texels on background *X* = *Gray*, there is little evidence that gray-scales differentially influence the activation of any light skin components on backgrounds *X* = *Black* or *X* = *Gray*. By contrast, on background *X* = *White*, The WS, WHB, WMB and WAT show significant differential sensitivity to gray-scale. In this context, the WHB-influence function shows a plausible pattern: *Black* and *Dark gray* (the gray-scales that differ most strongly from the *White* background) exert the strongest influence. Interestingly, on the *White* background for *c* = WS and *c* = WMB, the *c*-influence function assigns a lower value to *Light gray* than to the other four gray-scales. In particular, the WS-influence function assigns a value to *White* that is clearly higher than the value it assigns to *Light gray* even though *White* texels are invisible against the *White* background. We address the question of why this might be in the discussion. The WAT shows a

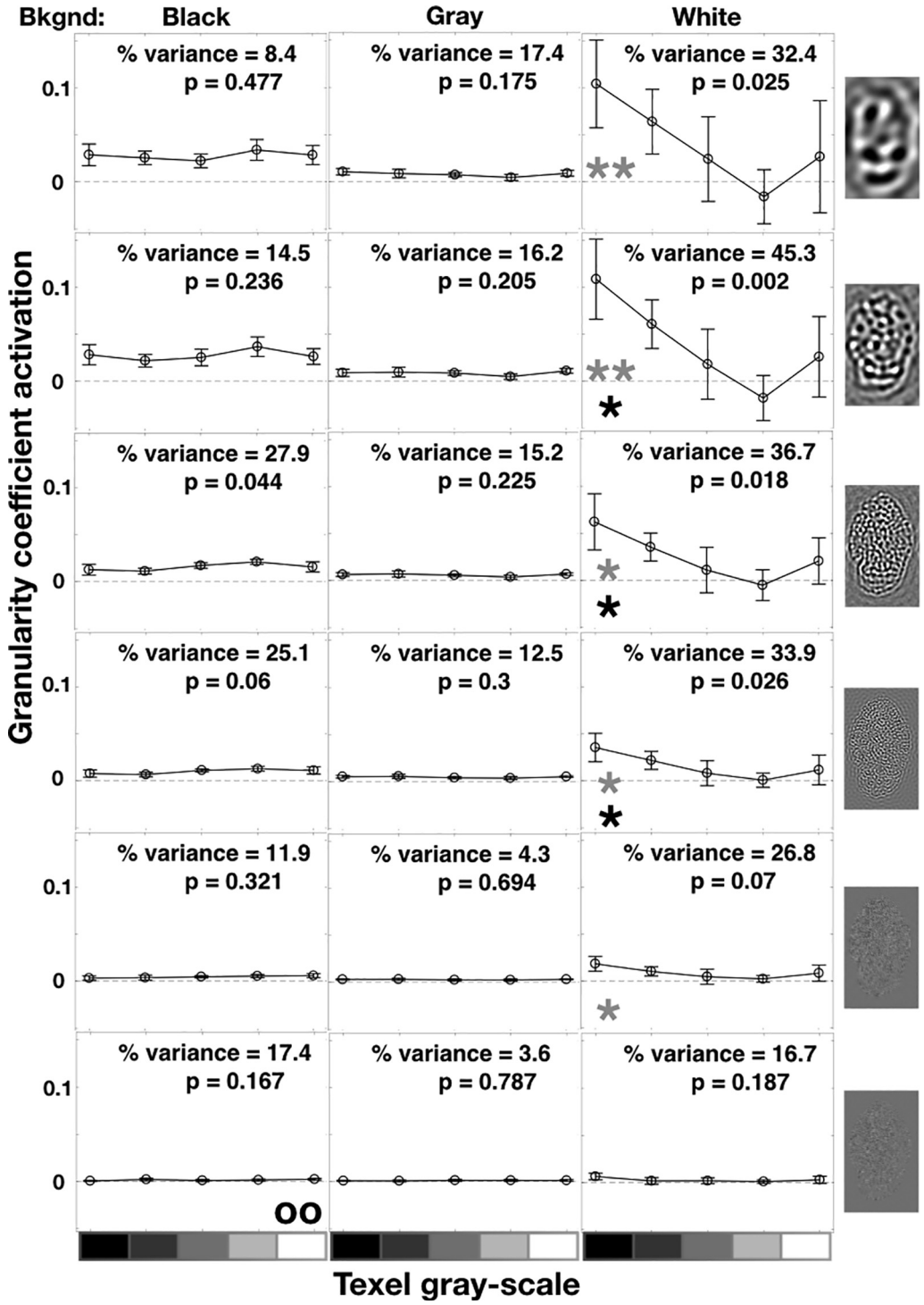

Fig. 11. *Results from Experiment 2 for granularity spectrum coefficients*. For a given coefficient *c* and background gray-scale *X*, the curve plotted in the panel in row *c* and column *X* gives the average *c*-influence function $\bar{f}(g)$ for g = *Black*, *Dark gray*, *Gray*, *Light gray*, and *White*. Within each panel, more positive values indicate increased sensitivity. Error bars are 95% confidence intervals. Black "oo" ('*') indicates that *White* (*Black*) texels influence *c*-activation more strongly than *Black* (*White*) texels at the 0.0031 (0.01) significance level. Gray "**" ('*') indicates that *Black* texels influence *c*-activation more strongly than *Light gray* texels at the 0.0031 (0.01) significance level. See "*Experiment 1 results*" for description of "*% variance*" and "*p*."

pattern of influence that differs strikingly from those of the WS, WHB and WMB. WAT-activation increases with increasing proportions of *Dark gray, Gray* and *Light gray* texels and decreases with increasing proportions of *White* and *Black* texels.

The results from Experiment 2 for the granularity spectrum coefficients are shown in Fig. 11. The most striking feature of Fig. 11 is that the differential influence of gray-scale on granularity spectrum coefficients is stronger on *White*-background scrambles than on *Black*- or *Gray*-background scrambles. In the *White*-background context, the *c*-influence functions for different granularity band coefficients *c* are all similar in form but differ in amplitude: like the WS- and WHB-influence functions, they assign higher values to *White* than they do to *Light gray* even though *White* texels are invisible against the *White* background in these substrates.

7.3. Higher-order effects

There was substantial evidence of higher-order effects. For the Bonferroni-corrected critical value of $p_{crit} = 0.05/16 = 0.0031$, the test for higher-order effects yielded $p < p_{crit}$ for (1) the White Mantle Bar, White Head Bar, and the anterior Transverse Mantle Bar in the *Black*-background context; (2) the White Square and the Anterior Transverse Mantle Bar in the *Gray*-background context; (3) the White Square, Anterior Transverse Mantle Bar and Posterior Transverse Mantle Bar in the *White*-background context. In addition, 8 other tests yielded $p < 0.01$.

We conclude that in the *Black*-, *White*- and *Gray*-background contexts, the simple linear model illustrated in Fig. 4 does not provide a complete description of cuttlefish patterning responses. The exact nature of the higher order effects implicated by these tests falls outside the scope of the current study.

8. Experiment 2 discussion

The most striking feature of the results from Experiment 2 is that differential influence of gray-scale on activation (both of skin components and also of granularity spectrum coefficients) is most pronounced in the context of *White*-background scrambles. The dark skin component, AHB, and light skin components WHB, WS and WAT all show significant differential sensitivity to gray-scales in the context of the *White* background. Only the WHB shows (marginally) significant differential sensitivity to gray-scale in the context of the *Black* background, and only the WS shows significant differential sensitivity to gray-scale in the context of the *Gray* background. In addition, each of the first four granularity spectrum coefficients shows significant differential sensitivity to gray-scale in the context of the *White* background. By contrast, only coefficients 4 and 5 show marginally significant sensitivity to gray-scale against the *Black* background, and none of the granularity spectrum coefficients show significant differential sensitivity to gray-scale against the *Gray* background.

The pattern of differential sensitivity to gray-scale in the context of the *White*-background is surprising, however, in the following sense: for c = WS, WHB and granularity spectrum coefficients 1, 2 and 3, the c-influence function hits its minimum value at *Light gray*. In particular, in many cases, the c-influence function assigns a significantly lower value to *Light Gray* than it does to *White* even though *White* texels are invisible against the *White* background.

There are at least two possible reasons for this effect. First, as the number of *White* texels is increased in a substrate with a *White* background, larger regions of the background are made homogeneously white. This increased background homogeneity may heighten the effective salience of the non-*White* texels in the substrate increasing the effectiveness with which they activate the pattern statistics c. Second, introducing *White* texels into a *White*-background substrate chops up the regularity of the square grid of texels. It is possible that this increased irregularity is itself a stimulus feature that operates to activate the pattern statistics c. Whether or not either or both of these factors underlie the current results is a question for future research.

Although there is little evidence of differential sensitivity to gray-scale in the context of the *Black* background, this should not be taken to imply that *Black*-background substrates fail to evoke disruptive pattern responses. Note in particular that even though the WS fails to show significant differential sensitivity to gray-scale against the *Black* background, the WS-influence function has an average value that is well above 0. This implies that the WS tends to be strongly but approximately equally activated by all of the *Black*-background substrates. The same is true of granularity spectrum coefficients 1, 2, and 3. This finding is consonant with Chiao & Hanlon, 2001a, 2001b, who showed that sparse *White* elements on a *Black* background evoke disruptive pattern responses provided they are roughly equal in area to the WS.

9. Concluding thoughts

Experiment 1 explored how different gray-scales influence pattern responses in the context of densely packed substrates. Substrate texel-area was varied over 4 sizes: 100%, 50%, 30% and 10% WS-area. Experiment 2 explored how differential sensitivity of pattern responses to gray-scale is affected by the background gray-scale against which texels appear. Three backgrounds were tested: *Black*, *Gray*, and *White*.

The results of both experiments underscore the importance of substrate elements of negative contrast polarity in controlling disruptive responding. Across all seven substrates X and all 16 skin pattern statistics c, paired-samples t-tests revealed that in 20 cases, *Black* texels were significantly more effective than *White* texels in activating c; by contrast, *White* texels were significantly more effective than *Black* texels in only 4 cases. Under the null hypothesis that *White* and *Black* texels are equally effective in controlling skin-pattern responses, the probability of observing such a large disparity between the number of significant results for *Black* vs. *White* texels is 0.0015. As indicated by the asterisks that mark 12 of the 20 panels (and the absence of circles) in Fig. 6, the dominance of *Black* vs. *White* texels in stimulating activation is especially pronounced for the light skin components in the context of the four densely-packed substrates. In Experiment 2, *Gray*-background substrates evoked little disruptive patterning, and although *Black*-background substrates (in which context all texels all have nonnegative contrast polarity) evoked strong disruptive pattern responses, these responses showed little differential sensitivity to gray-scale. By comparison, the responses evoked by *White*-background substrates (in which context all non-*White* texels have negative contrast polarity) showed substantial differential sensitivity to gray-scale.

We conclude that in the context of cluttered substrates, elements of negative contrast polarity predominate in controlling cuttlefish pattern responses. This finding echos results from human psychophysics (Chubb, Econopouly, & Landy, 1994; Chubb, Landy, & Econopouly, 2004; Chubb & Nam, 2000; Dannemiller & Stephens, 2001; Komban, Alonso, & Zaidi, 2011; Lu & Sperling, 2012; Whittle, 1986) which have demonstrated that human vision is highly asymmetric in its processing of negative versus positive contrast polarity with higher sensitivity to black than to white scene components. The current findings are also consonant with results from monkey neurophysiology (Jin, Wang, Lashgari, Swadlow, & Alonso, 2011; Xing, Yeh, & Shapley, 2010; Yeh, Xing, & Shapley, 2009) that suggest that area V1 of macaque primary visual cortex is wired to selectively amplify responses to black scene elements.

On the other hand, the current results are largely unanticipated by previous findings with cuttlefish (Chiao et al., 2015). Previous work has documented the importance, in the context of dense substrates, of spatial scale (Chiao et al., 2009) and pattern contrast (Barbosa et al., 2008a, 2008b) in controlling disruptive responding. Experiments using substrates with sparsely scattered items appearing against homogeneous backgrounds have demonstrated the importance of edges and edge-terminators in controlling disruptive responding (Chiao et al., 2013; Zylinski et al., 2009a, 2009b). Other studies have shown that the pattern painted on the surface of a 3-dimensional object (a cube) in the environment of the cuttlefish operates with special power (in comparison to the pattern painted on the rest of the substrate) to control cuttlefish response patterns (Buresch et al., 2011).

It should, however, be noted that in all of the work cited above, bright and dark scene elements were manipulated in yoked fashion: when pattern contrast is lowered, bright scene elements are darkened and dark scene elements are brightened simultaneously. Thus, none of those experiments could possibly have revealed the effects documented in the current study.

One previous experiment, however, is consonant with the current fundings. Chiao et al., 2010, manipulated the proportion of white vs. black elements in bandpass-filtered texture thresholded to produce dense, binary texture roughly matched in granularity to a cuttlefish

mottle pattern. In separate conditions, the threshold was set so that ¼, ½, or ¾ of the pixels in the resulting binary texture were black (the rest being white). It was found that the texture ¾ of whose pixels were black evoked significantly stronger disruptive responding than either of the other textures.

What might be the adaptive benefit of aligning disruptive pattern responses to the presence of *Black* and *Dark gray* elements in the context of cluttered environments? The most dramatic luminance variations in images of natural scenes are due to shading. Unshaded vs. shaded regions of equal reflectance in a single scene can easily differ by orders of magnitude in the light they project to the retina of a viewer. In the habitat of the cuttlefish, cluttered substrates are often random amalgams of shells, stones, plant material, etc. presenting a complex structure of occlusory boundaries between overlapping objects. Substantial research shows that disruptive pattern responses are strongly driven by the luminance edges typically produced by such boundaries (Chiao et al., 2013; Zylinski et al., 2009a, 2009b). Such boundaries are nearly always associated with local regions of dramatic shading that produce dark elements in the visual input. We hypothesize that in the cuttlefish habitat, in the context of high-variance visual input characteristic of cluttered substrates, dark elements reliably signal the presence of occlusory boundaries. It is precisely in the presence of rich arrays of such boundaries that disruptive pattern responses are likely to be effective (Cuthill et al., 2005; Stevens, Cuthill, Windsor, & Walker, 2006). We align with Stevens & Cuthill, 2006, in proposing that in such contexts, the WS and other skin components are activated primarily to generate false occlusory boundaries within the visual region subtended by the body of the cuttlefish, thereby enabling it to elude detection by visually dismantling itself into chunks of apparently overlapping detritus similar to the rest of the scene.

Acknowledgments

This work was supported in part by NSF Award DBI #1005378 to M.A.B. NSF Award BCS-0843897 to C.C., and the Sholley Foundation to R.T.H.

Appendix A. Supplementary data

Supplementary data associated with this article can be found, in the online version, at http://dx.doi.org/10.1016/j.visres.2018.06.003.

References

Allen, J. J., Mäthger, L. M., Barbosa, A., Buresch, K. C., Sogin, E., Schwartz, J., ... Hanlon, R. T., et al. (2010). Cuttlefish dynamic camouflage: Responses to substrate choice and integration of multiple visual cues. *Proceedings Biological Sciences, 277*, 1031–1039.

Allen, J. J., Mäthger, L. M., Barbosa, A., & Hanlon, R. T. (2009). Cuttlefish use visual cues to control three-dimensional skin papillae for camouflage. *Journal of Comparative Physiology A, 195*, 547–555.

Anderson, J. C., Baddeley, R. J., Osorio, D., Shashar, N., Tyler, C. W., Ramachandran, V. S., et al. (2003). Modular organization of adaptive colouration in flounder and cuttlefish revealed by independent component analysis. *Network, 14*, 321–333.

Barbosa, A., Allen, J. J., Mäthger, L. M., & Hanlon, R. T. (2012). Cuttlefish use visual cues to determine arm postures for camouflage. *Proceedings Biological Sciences, 279*, 84–90.

Barbosa, A., Litman, L., & Hanlon, R. T. (2008a). Changeable cuttlefish camouflage is influenced by horizontal and vertical aspects of the visual background. *Journal of Comparative Physiology A, 194*, 405–413.

Barbosa, A., Mäthger, L. M., Buresch, K. C., Kelly, J., Chubb, C., Chiao, C.-C., et al. (2008b). Cuttlefish camouflage: The effects of substrate contrast and size in evoking uniform, mottle or disruptive body patterns. *Vision Research, 48*, 1242–1253.

Barbosa, A., Mäthger, L. M., Chubb, C., Florio, C., Chiao, C.-C., & Hanlon, R. T. (2007). Disruptive coloration in cuttlefish: A visual perception mechanism that regulates ontogenetic adjustment of skin patterning. *Journal of Experimental Biology, 210*, 1139–1147.

Buresch, K. C., Mathger, L. M., Allen, J. J., Bennice, C., Smith, N., Schram, J., et al. (2011). The use of background matching vs. masquerade for camouflage in cuttlefish *Sepia officinalis*. *Vision Research, 51*, 2362–2368.

Chiao, C.-C., Chubb, C., Buresch, K. C., Barbosa, A., Allen, J. J., Mäthger, L. M., et al. (2010). Mottle camouflage patterns in cuttlefish: Quantitative characterization and visual background stimuli that evoke them. *Journal of Experimental Biology, 213*, 187–199.

Chiao, C.-C., Chubb, C., Buresch, K., Siemann, L., & Hanlon, R. T. (2009). The scaling effects of substrate texture on camouflage patterning in cuttlefish. *Vision Research, 49*, 1647–1656.

Chiao, C.-C., Chubb, C., & Hanlon, R. T. (2007). Interactive effects of size, contrast, intensity and configuration of background objects in evoking disruptive camouflage in cuttlefish. *Vision Research, 47*, 2223–2235.

Chiao, C.-C., Chubb, C., & Hanlon, R. T. (2015). A review of visual perception mechanisms that regulate rapid adaptive camouflage in cuttlefish. *Journal of Comparative Physiology A: Neuroethology, Sensory, Neural, and Behavioral Physiology, 201*, 933–934.

Chiao, C.-C., & Hanlon, R. T. (2001a). Cuttlefish cue visually on area – not shape or aspect ratio - of light objects in the substrate to produce disruptive body patterns for camouflage. *Biological Bulletin, 201*, 269–270.

Chiao, C.-C., & Hanlon, R. T. (2001b). Cuttlefish camouflage: Visual perception of size, contrast and number of white squares on artificial checkerboard substrata initiates disruptive coloration. *Journal of Experimental Biology, 204*, 2119–2125.

Chiao, C.-C., Kelman, E. J., & Hanlon, R. T. (2005). Disruptive body patterning of cuttlefish (*Sepia officinalis*) requires visual information regarding edges and contrast of objects in natural substrate backgrounds. *Biological Bulletin, 208*, 7–11.

Chiao, C.-C., Ulmer, K. M., Siemann, L. A., Buresch, K. C., Chubb, C., & Hanlon, R. T. (2013). How visual edge features influence cuttlefish camouflage patterning. *Vision Research, 83*, 40–47.

Chubb, C., Econopouly, J., & Landy, M. S. (1994). Histogram contrast analysis and the visual segregation of iid textures. *Journal of the Optical Society of America A, 11*, 2350–2374.

Chubb, C., Landy, M. S., & Econopouly, J. (2004). A visual mechanism tuned to black. *Vision Research, 44*, 3223–3232.

Chubb, C., & Nam, J.-H. (2000). The variance of high contrast texture is sensed using negative half-wave rectification. *Vision Research, 40*, 1695–1709.

Cuthill, I. C., Stevens, M., Sheppard, J., Maddocks, T., Párraga, C. A., & Troscianko, T. S. (2005). Disruptive coloration and background pattern matching. *Letters to Nature, 434*, 72–74.

Dannemiller, J. L., & Stephens, B. R. (2001). Asymmetries in contrast polarity processing in young human infants. *Journal of Vision, 1*, 112–125.

Hanlon, R. H. (2007). Cephalopod dynamic camouflage. *Current Biology, 17*, R400–R404.

Hanlon, R. T., Chiao, C.-C., Mäthger, L. M., Barbosa, A., Buresch, K. C., & Chubb, C. (2009). Cephalopod dynamic camouflage: Bridging the continuum between background matching and disruptive coloration. *Philosophical Transactions of the Royal Society of London. Series B, Biological sciences, 364*, 429–437.

Hanlon, R. T., Chiao, C.-C., Mäthger, L. M., Buresch, K. C., Barbosa, A., Allen, J. J., ... Chubb, C., et al. (2011). Rapid adaptive camouflage in cephalopods. In M. Stevens, & S. Merilaita (Eds.). *Animal camouflage: Mechanisms and functions*. Cambridge, U.K: Cambridge University Press.

Hanlon, R. T., Chiao, C.-C., Mathger, L. M., & Marshall, N. J. (2013). A fish-eye view of cuttlefish camouflage using in situ spectrometry. *Biological Journal of the Linnean Society, 109*, 535–551.

Hanlon, R. T., & Messenger, J. B. (1988). Adaptive coloration in young cuttlefish (*Sepia officinalis L.*): The morphology and development of body patterns and their relation to behaviour. *Philosophical Transactions of the Royal Society of London. Series B, 320*, 437–487.

Hanlon, R. T., & Messenger, J. B. (1996). *Cephalopod behaviour*. Cambridge: Cambridge University Press.

Holmes, W. (1940). The colour changes and colour patterns of *Sepia officinalis* L. *Proceedings of the Zoological Society of London A, 110*, 2–35.

Jin, J., Wang, Y., Lashgari, R., Swadlow, H. A., & Alonso, J.-M. (2011). Faster thalamocortical processing for dark than light visual targets. *The Journal of Neuroscience, 31*(48), 17471–17479.

Kelman, E. J., Baddeley, R. J., Shohet, A. J., & Osorio, D. (2007). Perception of visual texture and the expression of disruptive camouflage by the cuttlefish, *Sepia officinalis*. *Proceedings Biological Sciences, 274*, 1369–1375.

Kelman, E. J., Osorio, D., & Baddeley, R. J. (2008). A review of cuttlefish camouflage and object recognition and evidence for depth perception. *Journal of Experimental Biology, 211*, 1163–1757.

Komban, S. J., Alonso, J.-M., & Zaidi, Q. (2011). Darks are processed faster than lights. *The Journal of Neuroscience, 31*(23), 8654–8658.

Lu, Z.-L., & Sperling, G. (2012). Black-white asymmetry in visual perception. *Journal of Vision, : 12*. (10:8), 1–21.

Marshall, N. J., & Messenger, J. B. (1996). Colour-blind camouflage. *Nature, 382*, 408–409.

Mäthger, L. M., Barbosa, A., Miner, S., & Hanlon, R. T. (2006). Color blindness and contrast perception in cuttlefish (*Sepia officinalis*) determined by a visual sensorimotor assay. *Vision Research, 46*, 1746–1753.

Mäthger, L. M., Chiao, C.-C., Barbosa, A., Buresch, K. C., Kaye, S., & Hanlon, R. T. (2007). Disruptive coloration elicited on controlled natural substrates in cuttlefish, *Sepia officinalis*. *Journal of Experimental Biology, 210*, 2657–2666.

Maxwell, S. E., & Delaney, H. D. (2000). *Designing experiments and analyzing data*. Lawrence Erlbaum Associates Inc p 479.

Messenger, J. B. (2001). Cephalopod chromatophores: Neurobiology and natural history. *Biological Reviews, 76*, 473–528.

Shohet, A. J., Baddeley, R. J., Anderson, J. C., Kelman, E. J., & Osorio, D. (2006). Cuttlefish responses to visual orientation of substrates, water flow and a model of motion camouflage. *Journal of Experimental Biology, 209*(Pt 23), 4717–4723.

Shohet, A. J., Baddeley, R. J., Anderson, J. C., & Osorio, D. (2007). Cuttlefish camouflage: A quantitative study of patterning. *Biological Journal of the Linnean Society, 92*, 335–345.

Stevens, M., & Cuthill, I. C. (2006). Disruptive coloration, crypsis and edge detection in early visual processing. *Proceedings of the Royal Society of London. Series B*. http://dx.

doi.org/10.1098/rspb.2006.3556.
Stevens, M., Cuthill, I. C., Windsor, A. M. M., & Walker, H. J. (2006). Disruptive contrast in animal camouflage. *Proceedings of the Royal Society of London. Series B, 273*, 2433–2438.
Stubbs A. L. & Stubbs C. W. (2015) A novel mechanism for color vision: pupil shape and chromatic aberration can provide spectral discrimination for "color blind" organisms. bioRxiv: http://dx.doi.org/10.1101/017756.
Tublitz, N. J., Gaston, M. R., & Loi, P. K. (2006). Neural regulation of a complex behavior: Body patterning in cephalopod molluscs. *Integrative and Comparative Biology, 46*, 880–889.
Whittle, P. (1986). Increments and decrements: Luminance discrimination. *Vision Research, 26*, 1677–1691.
Xing, D., Yeh, C. I., & Shapley, R. M. (2010). Generation of black-dominant responses in v1 cortex. *The Journal of Neuroscience, 30*(40), 13504–13512.
Yeh, C. I., Xing, D., & Shapley, R. M. (2009). Black responses dominate macaque primary visual cortex v1. *The Journal of Neuroscience, 29*, 11753–11760.
Zylinski, S., Darmaillacq, A. S., & Shashar, N. (2012). Visual interpolation for contour completion by the European cuttlefish (*Sepia officinalis*) and its use in dynamic camouflage. *Proceedings Biological Sciences, 279*, 2386–2390.
Zylinski, S., Osorio, D., & Shohet, A. J. (2009a). Edge detection and texture classification by cuttlefish. *Journal of Vision, 9*, 1–10.
Zylinski, S., Osorio, D., & Shohet, A. J. (2009b). Perception of edges and visual texture in the camouflage of the common cuttlefish, *Sepia officinalis*. *Philosophical Transactions of the Royal Society of London. Series B, 364*, 439–448.
Zylinski, S., & Osorio, D. (2011). What can camouflage tell us about nonhuman visual perception? A case study of multiple cue use in the cuttlefish. In M. Stevens, & S. Merilaita (Eds.). *Animal camouflage: Mechanisms and functions*. Cambridge, U.K: Cambridge University Press.